Scramjet Engine/Airframe Integration Methodology

by

James L. Hunt and Charles R. McClinton
NASA Langley Research Center
Hampton, Virginia

1. ABSTRACT

Scramjet engine/airframe integration methodology currently in use at the NASA Langley Research Center for design/analysis of hypersonic airbreathing vehicles is presented with illustrative example applications. The matrix encompasses engineering and higher order numerical methods that cover the major disciplines as well as a multidiscipline design/optimization approach.

2. INTRODUCTION

The Systems Analysis Office (SAO) and the Numerical Applications Office (NAO) of the Hyper-X Phase I Program Office (HXPO)/Aerospace Transportation Technology Office (ATTO) at NASA Langley Research Center provide evaluation, analysis and design of hypersonic airbreathing vehicles for both industry and government. A wide range of vehicles and missions are investigated, including single-, two-, and three-stage-to-orbit vehicles, as well as endoatmospheric cruise and accelerator vehicles (fig. 1, ref. 1). For all these vehicles, the forebody acts as an external inlet, precompressing air for delivery to the dual-mode scramjet inlet/combustor and the aftbody acts as an external nozzle for the expansion of exhaust gases. The result is a propulsion system that is totally integrated from nose to tail, and thus it is a major shaping influence on the design of the vehicle. Due to the highly integrated engine/airframe and the extensive flight envelope inherent in airbreathing hypersonic vehicle design, analyses of these vehicles involve many interdependent disciplines with high sensitivities among the large set of design variables and a highly nonlinear design space. It is therefore necessary to resolve most airbreathing hypersonic vehicles to a preliminary design level, even for those that would traditionally be considered as conceptual design. With this amount of detail required as well as the requirement for a short

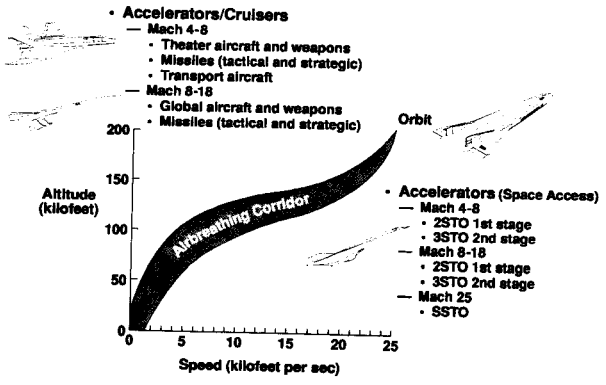

Figure 1. Hypersonic airbreathing vehicle design matrix.

design response time, analysis methods have been developed and improved to provide both rapid and accurate results. The stable of software tools span engineering and computational fluid dynamics (CFD) methods.

In order to minimize vehicle characteristics such as fuel fraction for performing a mission and resultant gross/dry weight, the airframe integrated subsonic/supersonic combustion ramjet should have at least four desirable features. First, the installed performance of the engine should be maximized over the Mach number range of operation; second, the engine integration should be such that the effective specific impulse of the vehicle is maximized over the accelerated portion of the trajectory; third, the engine should be able to be regeneratively cooled (except for missiles); and fourth, the engine should be light weight. These features should accrue in either a fixed geometry or highly variable geometry engine architecture or something in between. In addition, the subsonic/supersonic combustion ramjet/scramjet must have inlet and nozzle shapes that are conducive to airframe integration. The large nozzle area relative to freestream capture area requirements for hypersonic speeds necessitates integrating the engine with the airframe in order to use the afterbody of the vehicle as the engine nozzle and thereby minimizing the cowl drag. Vehicle design considerations in hypersonic flow show that the reliable prediction of a dual-mode scramjet performance is an absolute must in resolving hypersonic airbreathing vehicle designs. This becomes evident upon consideration of the fact that the net thrust for these vehicles is a relatively small difference between two large forces, the nozzle thrust and the forebody ram drag; thus, the potential for error and resultant sensitivity is high.

Because of the significance of the ramjet/scramjet integration on the design of hypersonic airbreathing vehicles, this paper focuses on the dual-mode ramjet engine/airframe integration methodologies currently in use in the SAO and the NAO and the enhancements in progress and those planned. Engineering and CFD methods to insure the evolution of engine/airframe integrated dual-mode ramjet designs with the desirable features mentioned above are discussed.

3. PROPULSION FLOWPATH/FORCE ACCOUNTING

For an underslung ramjet/scramjet airframe-integrated vehicle in which the vehicle lower forebody acts as a precompression surface and the vehicle lower aftbody acts as a high expansion ratio nozzle, the entire undersurface of the vehicle is a propulsion flowpath. This propulsion flowpath is defined by those surfaces that are wetted by air that flows through the engine nacelle and the forces acting thereon are charged to

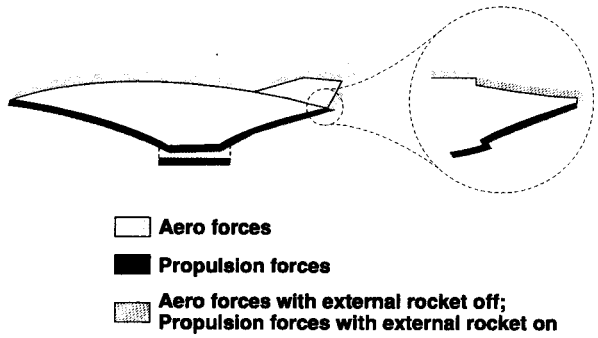

Figure 2a. Cowl-to-tail force accounting system.

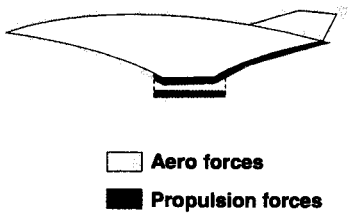

Figure 2b. Cowl-to-tail force accounting system.

propulsion (fig. 2a). This includes the lower external forebody, the interior nacelle, and the exterior nozzle aftbody. Forces on all other exterior surfaces including the exteriors of the engine cowl and sidewall are charged to aerodynamics. This classic force accounting system is referred to as freestream-to-freestream or more commonly nose-to-tail. When the engine is not operating (e.g., during reentry), exterior forebody and nozzle forces are charged to aerodynamics.

A second force accounting system, known as cowl-to-tail, is shown in figure 2b. Here, the propulsion accounting begins at the cowl lip rather than the apex of the vehicle and proceeds through the engine and out the aftbody nozzle. This approach usurps the need to trace streamlines forward from the cowl lip to the freestream in order to define the forebody control volume in the nose-to-tail accounting system and gives the aerodynamics a more conventional role that now includes the lower forebody.

If a control volume (momentum balance) cycle analysis approach is used to resolve the forces in the propulsion flowpath as depicted in figure 3a, then additional propulsion related forces should be designated which do not represent actual forces acting on the vehicle propulsion flowpath surfaces but rather are a result of the way in which control volumes are defined. These are: (1) spillage drag due to shock losses associated with uncaptured spilled air (fig. 3a); (2) plume drag which is a fictitious drag captured by the control volume at the external nozzle flow interface with the freestream flow (a virtual surface, fig. 3a) and thus must be added back into the force accounting; (3) ram drag which is the stream-thrust at the forward control volume interface with the forebody flow (subsequently captured); and (4) nozzle gross thrust which is the stream-thrust at the nozzle exit control volume interface. At the time that this approach was first implemented in hypersonic propulsion cycle analysis, only forces in the flight direction were of interest; effective specific impulse, Isp was the primary focus. The control volume approach could not adequately predict propulsive lift and pitching moment, so an improved method was needed.

In propulsion cycle analysis methods that integrate the pressures on the propulsion surfaces in contrast to the control volume and momentum balance approach, none of the above corrections are required. This also applies to hybrid schemes (ref. 2) in which a control volume is used only for the combustor force resolution, and wall pressure plus skin friction integration's are used to resolve the forces on the remainder of the flowpath surfaces. Consequently, hybrid schemes lend themselves very well to propulsive lift and pitching moment computations. Figure 3b illustrates a hybrid scheme. This approach has become more practical in recent history due to improvements in computational technology. Thus, in general, forces resolved from control volumes confined to interior surfaces require no virtual interface corrections.

4. CLASSES OF METHODS

Scramjet engine/airframe integration methodology can be classified into four levels (fig. 4. ref. 3). Level 1 uses analytical methods and generally include iteration on closed form solutions which are coded into fast running computer programs. Level 2 makes the transition to numerical analysis and includes finite difference/element/volume inviscid (Euler) flow field analysis and heat conduction/transfer codes. Also included in Level 2 are the integral boundary layer codes and finite element stress analysis codes. Levels 1 and 2 constitute the engineering methodology category since they are used extensively in conceptual/preliminary design and performance tasks. Level 2 also includes hybrid methods which combine and integrate methodologies across the fluid-structural-thermal disciplines.

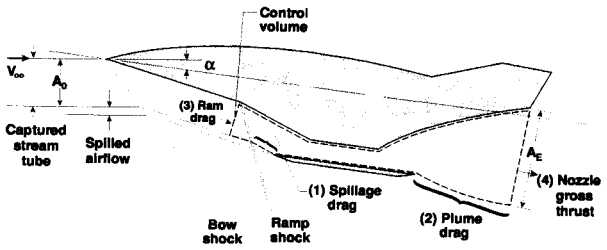

Figure 3a. Propulsion flowpath, control volume, and vectoral relationships—traditional approach.

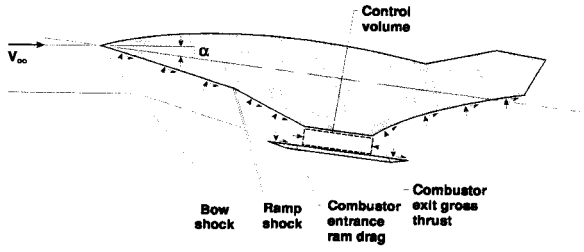

Figure 3b. Propulsion flowpath, control volume, and vectoral relationships—hybrid approach.

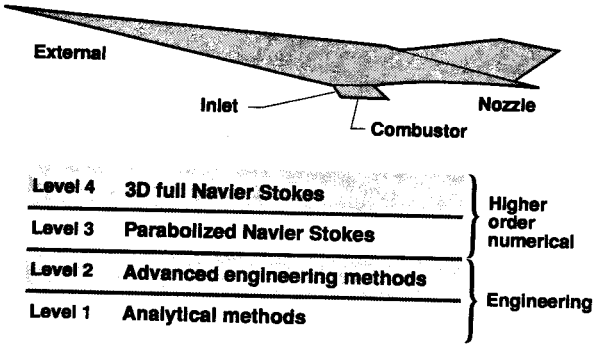

Figure 4. Methodology classification levels.

Level 3 consists of the Parabolized Navier Stokes (PNS) finite difference/volume codes which are used for parabolic problems. These flows generally consist of large supersonic regions with only embedded subsonic pockets. Level 4 is the highest level of analysis and consists of time-averaged Navier Stokes (TANS) codes. These can be Full Navier Stokes (FNS) codes or Navier Stokes solutions using the thin layer approximation (TLNS). These are used for flows which are viscous dominated and elliptic in nature, i.e. downstream pressure feed-back effects are included. The NS codes allow shear stress and heat transfer to be computed directly. Also included in Level 4 are the new coupled multi-disciplinary codes which include significant interaction among the fluid-structure-thermal effects.

Do not be confused by the levels. More is not always better. PNS is completely appropriate for some flows, those which have no separation. Engineering methods are also best for preliminary trade studies.

4.1 Engineering Methods

Engineering methods constitute the Level 1 and 2 classes of methodologies. They are used primarily in conceptual/preliminary design and performance tasks.

4.1.1 Cycle Analysis

The ramjet/scramjet cycle code used for characterizing performance as well as refining flowpath design for highly integrated engine/airframe configurations in SAO/NAO is SRGULL (fig. 5, ref. 2). SRGULL was developed at Langley

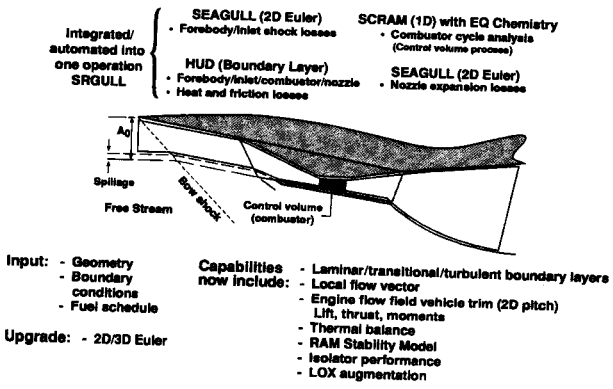

Figure 5. Tip-to-tail scramjet/ramjet cycle analysis, SRGULL.

over the last twenty five years by S. Z. Pinckney. It accurately resolves the net propulsive thrust of an airbreathing vehicle as a small difference between the combustor/nozzle thrust and the forebody/inlet drag. The forebody flowfield properties and the mass capture which SRGULL predicts are critical in resolving the net thrust.

SRGULL uses a 2-D/axisymmetric Euler (finite-difference, shock fitting) algorithm on the forebody and inlet, coupled with a boundary-layer solution, to predict the forebody/inlet drag and the flow properties entering the engine. The ramjet/scramjet solution is then completed using a 1-D cycle analysis with equilibrium chemistry and multiple steps through the combustor. A fuel mixing distribution with length is required input. Finally, the nozzle forces are resolved using the 2-D Euler and boundary-layer codes. A 3-D Euler capability is now being implemented into the code.

Capabilities in the SRGULL code include the analysis of laminar, transitional, and turbulent boundary layers; engine flowpath forces such as lift, thrust, and moments; and LOX augmentation of the scramjet which consists of small rocket motors firing parallel to the flow just downstream of the throat either at stoichiometric, fuel-rich or fuel-lean conditions. To first order, a thermal balance can also be accomplished. Given the wall temperature, heat flux to the walls (calculated by the code) and the fuel injection temperature, the amount of fuel required to actively cool the vehicle is determined. This fuel flow rate is then used to predict the net thrust for a thermally balanced system. Particularly at high hypersonic flight Mach numbers, the increased fuel flow rate, which is generally above an equivalence ratio of one, can significantly increase thrust but decreases specific impulse. The prediction of coolant fuel flow rate is further refined in the thermal management analysis as described in the corresponding section below.

SRGULL (ref. 2) also has the capability to predict engine unstart (ref. 4), which is another unique feature of this cycle code. Figure 6 (ref. 4) shows an isolator/ramjet/scramjet keelline at the top. The arrows mark points where fuel can be injected. The four plots show the pressure distribution through the engine as a function of distance along the engine for various freestream Mach numbers where transition between pure ramjet and pure scramjet occurs. Note that in the top plot, fuel is being injected from the middle injectors at an equivalence ratio of 0.3 and from the downstream injectors at an equivalence ratio of 0.7. Also note the rise in pressure that occurs upstream of the $\phi = 0.3$ fuel injector. If more fuel were to be added at this fuel injector, the pressure rise would be pushed farther and farther upstream, until at some point an engine unstart occurs. Note that as the freestream Mach number increases, the fuel can be injected farther upstream without causing the disturbance to move upstream.

Figure 7 (ref. 4) shows an experiment run in a Langley tunnel to study the effects of geometry changes on isolator flowfield characteristics. As shown, SRGULL accurately predicts the pressure disturbance in the isolator.

The NASP Concept Demonstrator Engine (CDE) was tested in the 8-ft. diameter High Temperature Tunnel (HTT) at

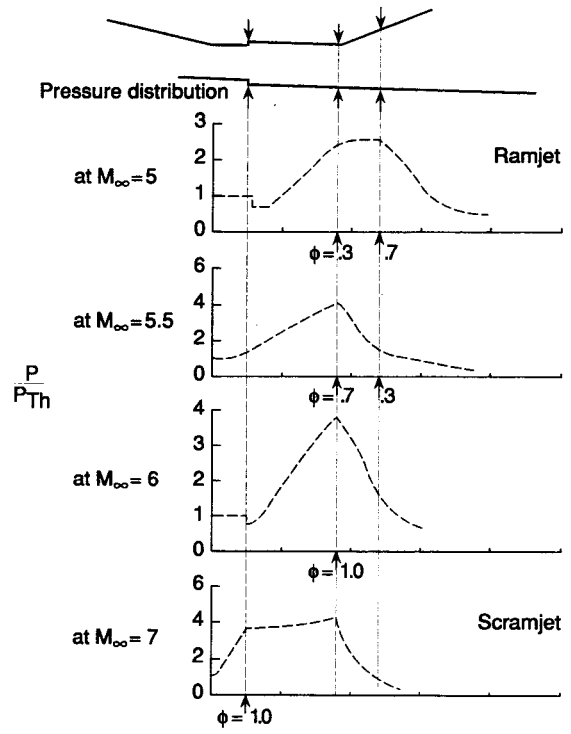

Figure 6. Ramjet to scramjet mode transition with SRGULL.

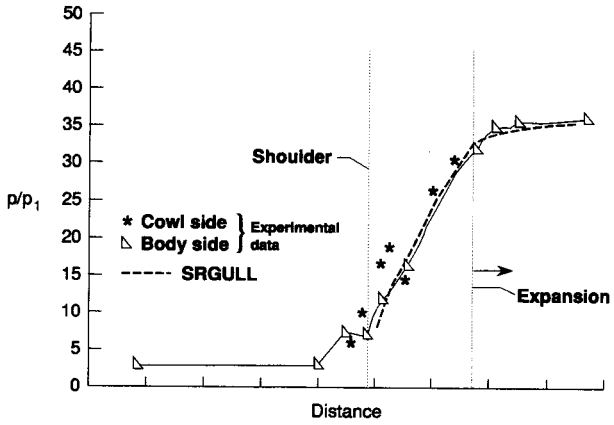

Figure 7. Isolator model comparison with Mach 4 experimental data.

Langley. SRGULL accurately predicted the flowpath pressure distribution, including the pressure-rise magnitude and location, of the CDE in the 8' HTT at Mach 7 test conditions.

4.1.2 Inviscid Flow

Euler codes are used to approximate these flows in support of flowpath design/performance for underslung engine/airframe integrated configurations in which forebodies precompress the air entering the inlet and aftbodies provide combustor flow expansion surfaces.

4.1.2.1 2-D/Axisymmetric Euler

The 2-D/axisymmetric Euler code used in SAO/NAO is SEAGULL (ref. 5). It was developed by Manual Salas at Langley in the mid 70's. It is a floating shock fitting technique in which second-order difference formulas are used for the computation of discontinuities. A procedure, based on the coalescence of characteristics is used to detect the formulation of shock waves. Mesh points that are crossed by discontinuities are recomputed. The technique provides resolution for 2-D external or internal flows with an arbitrary number of shock waves and contact surfaces. An example solution for the inviscid flow internal to a 2-D scramjet is presented in figure 8.

4.1.2.2 3-D Euler

To resolve 3-D inviscid flows, an unstructured, adaptive mesh Euler code (SAMflow, ref. 6) has been implemented in SAO/NAO by Dr. M. K. Lockwood. The unstructured, adaptive mesh methodology (ref. 7) was selected to provide resolution of shocks in a capturing technique with minimum gridding effort by the analyst.

The spatial discretization is accomplished via finite element techniques on unstructured tetrahedral grids. In order to achieve high execution speeds, edge-based data structures are used. Either central or upwind flux (van Leer, Roe) formulations can be used. For the temporal discretization, both Taylor-Galerkin and Runge-Kutta time integration schemes are available. Monotonicity of the solution may be achieved through a blend of second- and fourth-order dissipation, Flux-Corrected Transport (FCT), or classic Total Variational Dimensioning (TVD) limiters. The equations of state supported by SAMflow include ideal gas, polytropic gas and real air table look-up.

A variety of boundary conditions can be prescribed to simulate engineering flows: subsonic, transonic, and supersonic in/outflow boundary conditions, total pressure inflow boundary conditions, static pressure, Mach number and normal flux outflow boundary conditions, and porous walls and periodicity boundary conditions.

An example application is shown in figure 9 in which the SAMflow code is used to resolve the 3-D nose-to-tail inviscid flow on a Mach 10, lifting-body airplane. These calculations were used to quantify the 3D inlet and nozzle flows in a dual-fuel lifting body configuration development study (ref. 8).

Also, the methodology (ref. 7) includes the capability for treating moving boundaries with prescribed motion or moving rigid bodies with motion computed from six degree of free-

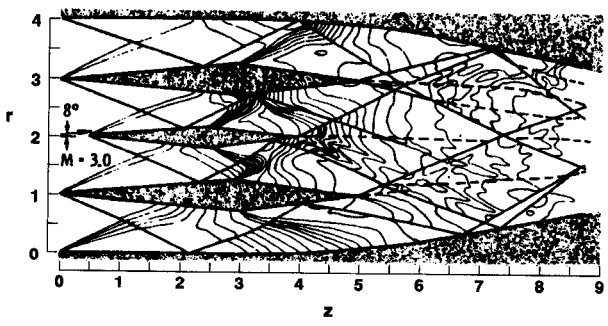

Figure 8. Flowfield for a simulated scramjet, showing shock waves, vortex sheets and isobars.

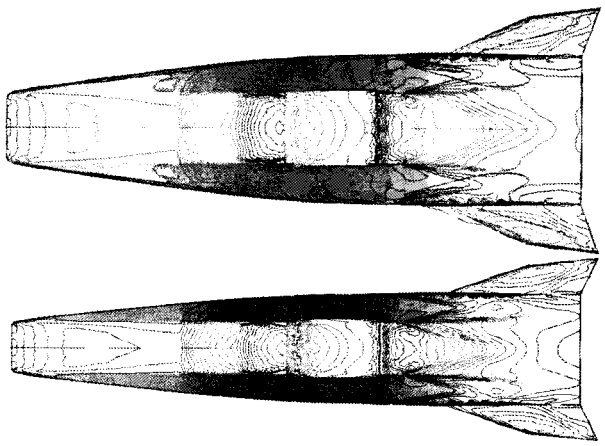

Figure 9. 3-D inviscid pressure contours on lifting-body cruise configuration at Mach 10 (design point) for two fineness ratios.

dom mechanics based on aerodynamic forces which are then linked back to the flow solver. To this end, the equations that constitute SAMflow are solved in the Arbitrary Lagrangean-Eulerian (ALE) frame. It is from this perspective, in addition to steady state solutions, that SAMflow is being used to assist in resolving the Hyper-X staging/separation flow/dynamics.

4.1.3 Boundary Layer

Boundary-layer calculations are required in the propulsion flowpath in conjunction with inviscid flow predictions to quantify heat transfer, skin friction (shear) and displacement thicknesses. For engineering calculations, SAO/NAO relies on integral methods.

In the cycle calculation, SRGULL (ref. 2), the basic integral method used (ref. 9) is applicable to the prediction of axisymmetric and two-dimensional laminar and turbulent boundary layers. It requires the simultaneous solution of the integral momentum, moment of momentum, and energy equations. In order to obtain this simultaneous solution, auxiliary relations are used for the boundary-layer velocity and enthalpy profiles, the shear distribution across the boundary layer, and the local surface friction and heat transfer, all of which are derived to be a function of the local pressure gradient and the total heat removed from the boundary-layer forward of the local station. These relations are derived using modified flat-plate log-log type velocity profiles for pressure gradients as a basis of departure from flat plate solutions (ref. 9), modified flat-plate Crocco-type enthalpy-velocity profile (ref. 10) to account for the total heat removed from the boundary layer, and flat-plate friction and heat transfer methods (Reynolds analogy). For laminar boundary layers, the flat-plate friction correlation method used is a combination of the Blasius incompressible friction coefficient correlation (ref. 11) and Eckert's reference temperature method for the compressibility correction (ref. 12). For turbulent boundary layers, the flat-plate friction correlation method used is the modified Spalding-Chi method of Neal and Bertram (ref. 13). For the heat transfer, the flat-plate method is the modified Reynolds analogy of Colburn (ref. 14).

For more general applications, boundary-layer predictions are calculated with a Boundary-Layer Integral Matrix Procedure (BLIMP, ref. 15). This well-known/widely used code was developed through U.S. Air Force funding to compute viscous boundary-layer effects over 2D axisymmetric or planar conditions as inputs. SAO/NAO results from the Euler solver SAMflow (ref. 6) is used to provide boundary-layer edge conditions to BLIMP. The edge conditions are supplied along inviscid streamlines along which the integral BLIMP procedure parabolically marches. This provides a reasonable merging of the accuracy of SAMflow for 3D inviscid flowfield computations and the reliability of BLIMP for viscous computations. In this manner, boundary layers on 3-D configurations (propulsion flowpath or aerodynamic surfaces) can be approximated; streamline divergence is included but without boundary-layer crossflow. An example of the coupled SAMflow-BLIMP software application on a hypersonic configuration in terms of pressure contours and heat transfer/shear stress distribution at Mach 2 is given in figures 10a and 10b respectively.

4.1.4 Thermal Management

The thermal management approach used for hypersonic air-breathing vehicles in SAO was developed by D. H. Petley and associates (ref. 16) and is based on a 3-D transient thermal analyzer (SINDA-85, ref. 17). It has been deemed the "Integrated Numerical Methods for Hypersonic Aircraft Cooling Systems Analysis" and includes capability for Thermal Protection System (TPS) sizing (ref. 18). The focus here is the propulsion flowpath.

Generally it is known a priori that the engine flowpath requires active cooling. An example of a coolant routing along the keel-line of the inlet, combustor and nozzle on the body

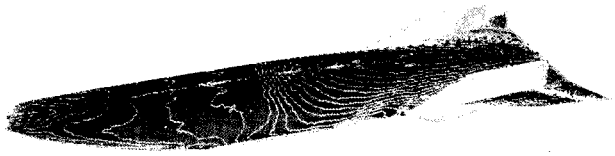

Figure 10a. SAMFLOW-generated surface pressure contours for a hypersonic cruise vehicle design.

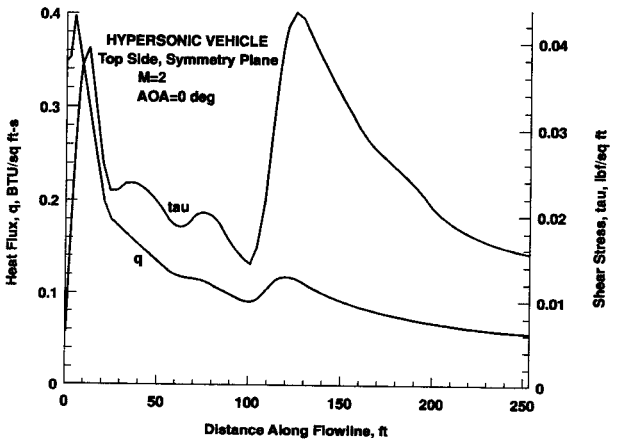

Figure 10b. BLIMP-generated heat flux and shear stress along top centerline for a hypersonic cruise vehicle design.

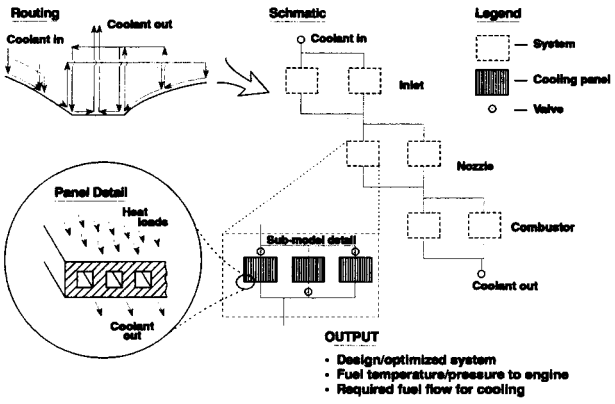

Figure 11. Cooling system design/analysis.

side of the propulsion flowpath is shown in the upper left-hand corner of Figure 11. Schematically, the active cooling network is shown in the middle of the figure. Inputs to the network analysis include the initial coolant system architecture, propulsion heat loads and flowpath geometry, coolant supply temperature, coolant and material properties, and the total pressure drop through the network, based on the pumping system and the desired fuel injection pressure. From this, the coolant mass flow, temperature and pressure distribution, along with the panel temperature distribution are determined. The panel temperatures are checked to ensure that they remain below the material temperature limits. Also, panel stresses are calculated. For example, if a hole is punctured in one of the cooling panel walls, the stress on that wall must not be high enough to cause the panel to "un-zip." The network architecture and panel designs are modified until the overall cooling system weight and coolant flow rate are minimized, while meeting the above constraints. As noted in the propulsion section, the coolant flow rate and the fuel injection properties have a significant impact on the net propulsive thrust.

As an example, consider the cooling network design for the Access to Space airbreathing/rocket SSTO vehicle (ref. 19). Slush hydrogen was stored in the tank at 20 psig and 25° R. It was pumped to 5500 psi and 60° R before circulating through the cooling panels, then through a turbine to drive the pump, back into the cooling network again, and out into the combustor. The heat exchangers were sized at Mach 15 conditions, where the heat loads were the greatest. The cooling panel network was designed to deliver hot hydrogen to the injectors. Detailed thermal and fluid analysis was conducted on the cooling panels to determine the channel dimensions, pressure drop across each panel, and material selection.

4.1.5 Structures

Hypersonic vehicle structures are characterized by thermal loads that are as high as the mechanical loads; for portions of the propulsion flowpath, the thermal loads can be even higher than the mechanical loads. Due to the design sensitivities inherent in airbreathing hypersonic vehicles, it is necessary to accurately predict structural weight, as well as the aerothermoelastic flight response of the vehicle even at the conceptual/preliminary design level. Some of the codes used in the SAO include Pro/ENGINEER (ref. 20) for computer aided design, MSC/NASTRAN (ref. 21), P3 PATRAN (ref. 22), and Pro/MECHANICA (ref. 23) for finite element analysis to predict element loads; and an in-house developed software package, ST-SIZE (ref. 24), to perform panel failure mode analysis and panel sizing.

The automated structural design process (ref. 24), developed under the supervision of P.L. Moses, a non-personal services (NPS) contractor to SAO, is shown schematically in figure 12. This figure illustrates how a structural panel is sized in ST-SIZE (ref. 24). Starting on the left-hand side of the figure, initial element stiffnesses, thermal coefficients, thermal and mechanical loads, and the finite element geometry are input into the finite element analysis code. Forces on each of the elements are then determined. Moving to the right of the figure, the element forces, material selections and panel and beam concepts are input to the ST-SIZE code. Here up to 30 failure mode analyses in strength and 26 failure mode analyses in stability are performed, and the panel is sized to meet these failure modes. Given the new panel design, the element stiffnesses and thermal coefficients change and the FEA must recalculate the element forces. This iterative process continues until convergence is achieved. The net result is the minimum panel weight, which results from a maximally stressed panel that also meets each of the failure mode tests, all with the margin-of-safety.

In general, the structural panels of airbreathing hypersonic vehicles are unsymmetric—geometrically and/or thermally. As a result, traditional 2-D panel methods, which do not account for panel asymmetry, can predict inaccurate panel sizes. In contrast, an enhanced version of ST-SIZE, developed in SAO (ref. 25), models the panel asymmetry. This is accomplished by calculating the membrane bending coupling in the 2-D element. The methods of ST-SIZE are the basis for the HyperSizer™ code which is a commercial product of Collier Research and Development Corporation (ref. 25).

The unit weights of the engine primary structure for the Access to Space airbreathing single-stage-to-orbit (SSTO) vehicle (ref. 19) were the results of FEM analysis and automated structural design using the structural/thermal sizing code, ST-SIZE. The primary structure for supporting the propulsion flowpath operating pressure loads was a system of

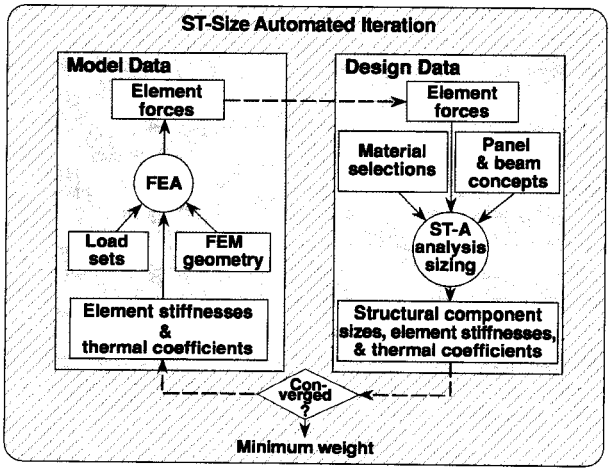

Figure 12. Structural sizing process.

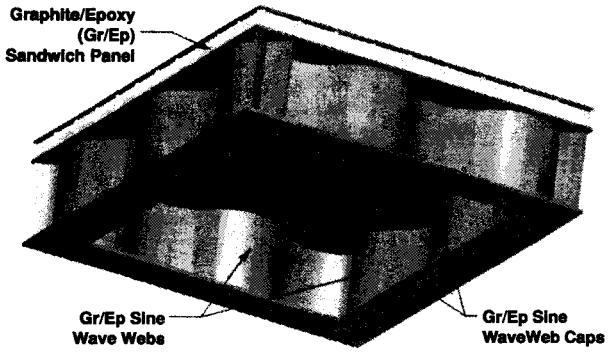

Figure 13. Primary structure concept for engine of SSTO vehicle.

honeycomb panels, backed by integrally attached stiffening beams made up of sine-wave webs and flat caps, as shown in Figure 13. This arrangement transmits the engine forces into trusses which are directly attached to the integral tank structure of the airframe. These trusses also provide stiffness to the airframe and naturally invoke some load sharing. The primary structure of the engine is isolated from the hot gas in the flowpath by non-integral heat exchangers that transmit the pressure forces through to the honeycomb panels.

4.2 Higher Order Numerical Methods

Resolution of the scramjet propulsion flowpath in preliminary to final design activities, and especially the resolution of mixing and combustion in the combustor requires the most sophisticated, more computationally intensive and less stable numerical methodologies of Level 3 and 4. These high fidelity approaches with suitable modelings of turbulence, viscous effects, and chemistry are the full Navier Stokes (elliptic) and parabolic Navier Stokes (marching) codes that capture both the inviscid and viscous flow characteristics simultaneously.

4.2.1 Full Navier Stokes

The code most relied on in NAO to resolve the most complex problems in the flowpath from 3-D shock/boundary-layer interaction in the inlet to fuel injection and mixing modeling in the combustor to 3-D expansion and possible relaminarization in a chemically reacting nozzle is the GASP code (General Aerodynamic Simulation Program, ref. 26 & 27). It was developed to provide generalized numerical predictions, encompassing flows over aerodynamic and propulsion-flowpath surfaces, that are required for the detail of hypersonic airbreathing vehicles.

GASP is a finite volume, upwind-biased code that can solve 1-dimensional, 2-dimensional, axisymmetric and fully 3-dimensional flows (ref. 28). It has various chemical and thermodynamic models for solving (single or multiple species) perfect gas flows, flow in chemical equilibrium, chemically frozen flows, and flows with finite chemical reactions. It can be run in the Space Marching (time-dependent parabolized Navier Stokes) or elliptic mode, either implicit or explicit, with Euler, Thin-Layer Navier Stokes (TLNS), and Full Navier Stokes (FNS) terms. Turbulence is modeled by either the standard algebraic Baldwin-Lomax model, a high Reynolds Number model for shear flows, or a choice of two 2-equation turbulent models that integrate completely through the boundary layer: The Lam-Bremhorst model (ref. 29) and Chien's model (ref. 30).

The GASP code is versatile (ref. 31) because of multi-block and multi-zone features and convenient to use for solving complex flowfields. The ability to switch from solving the full Navier- Stokes equations (elliptically) to the parabolized Navier-Stokes equations (in the marching mode) at any streamwise location in the computational domain makes it very convenient and efficient to use.

GASP is routinely utilized for analysis of scramjet component and engine flowpath performance. Figure 14 illustrates one such solution, for a powered wind tunnel model tested at NASA LaRC. This type of analysis provides comparison with experimental data. Comparison with the experimental data provides confidence in predicted flight vehicle engine performance. The GASP code has also been compared with simple "unit" inlet, combustor and nozzle experimental data bases. Figure 15 represents calibration (ref. 28) of the GASP turbulence modeling for nozzle heat transfer. This study demonstrated the requirement for a two-equation turbulence modeling for nozzle "relaminarization" effects on heat transfer. Similar studies have illustrated turbulence modeling requirements for the inlet shock boundary-layer interactions (ref.

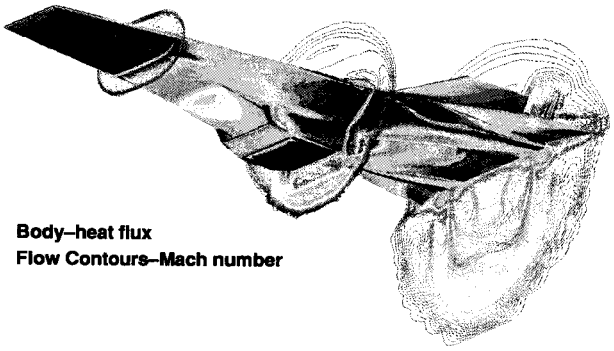

Figure 14. Powered hypersonic (Mach 7) vehicle CFD solution.

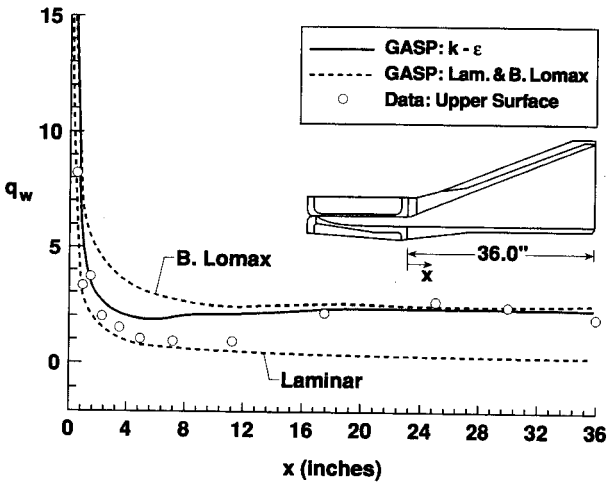

Figure 15. Heat transfer comparisons on nozzle upper surface.

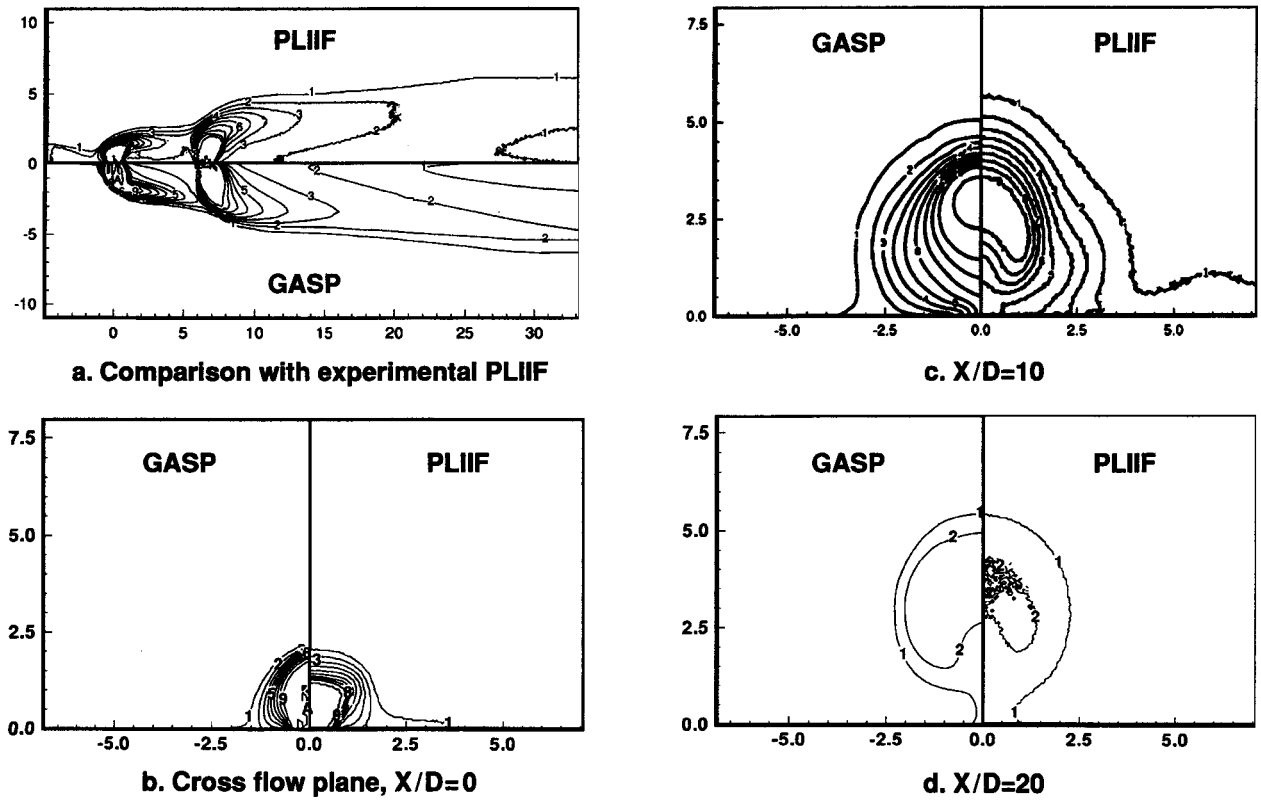

Figure 16. Comparison of injectant mole fraction contours on a flat plate from GASP solutions with experimental PLIF images.

32), including flow separation modeling, and grid resolution for shock-shock interaction cowl leading edge heat flux resolution. The GASP code has also been extensively verified for combustor analysis. An example of this is presented in figure 16 (ref. 31). This comparison with the University of Virginia (ref. 34) in-line flush wall injector, Planar Laser Induced Fluorescence (PLIF) data demonstrated that the GASP code can accurately predict the complex fuel mixing process. Similar comparisons have been made for cold and reacting flows at conditions up to flight Mach number 17 simulation (for example, ref. 35). In addition, GASP has been used to study facility effects on scramjet combustor performance (ref. 33). Figure 17 illustrates a solution for a cavity flame holder (ref. 36), which provided both fuel mixing and combustion efficiency, and evaluation of the combustor wall heating.

4.2.2 Parabolic Navier Stokes

PNS or space marching solutions are adequate for much of the scramjet flowpath, including large regions of the forebody and all of the nozzle. Design and analysis of scramjet fuel injection, mixing and combustion is one of the best uses for 3-D CFD methods. This process cannot be modeled with simpler methods, as the flow will always be three-dimensional. Effective design evaluation of scramjet combustor performance requires a rapid, approximate method for screening of concepts. The SHIP (Supersonic Hydrogen Injection Program) was developed for that purpose. The scramjet combustor, being predominantly supersonic flow, can be approximated using either space marching (GASP) of PNS (SHIP) solutions. The small subsonic regions are approximated by wakes, established by forcing the flow downstream, as described in reference 37. The SHIP3D code solves the parabolized, Favre averaged equations for the conservation of mass, momentum, total energy, total fuel and turbulence fields in a variable area domain of rectangular cross section (ref. 38). Turbulence closure is at the two-equation level, with one of several high-Re or low-Re models, including corrections for compressibility. The governing transport equations are solved by the SIMPLEC pressure correction algorithm (ref. 39) extended to compressible flow.

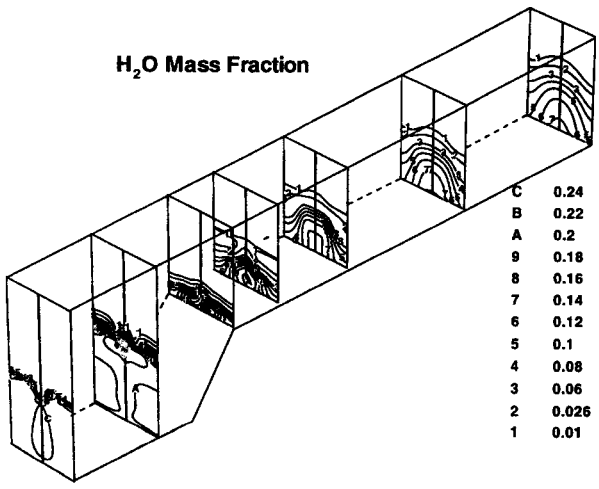

Figure 17. Water mass fraction from GASP for flame holding cavity injector.

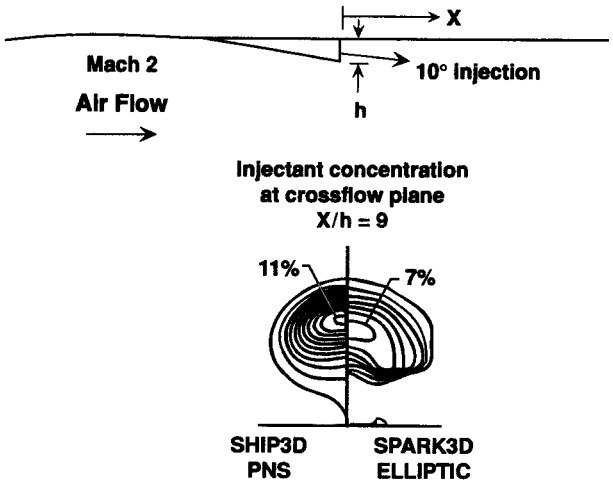

Figure 18. SHIP-SPARK comparison for ramp injection.

Figure 18 illustrates a comparison between fuel plume from a ramp-type fuel injector, predicted with a full Navier Stokes code, and with the SHIP PNS code. The SHIP code is routinely used for evaluation of scramjet combustor design options, including the effects of fuel and film/transpiration injector design, combustor expansion effects on mixing, etc. Parametric combustor design studies are possible with the SHIP code, an example of which is presented in reference 40.

5. DISCIPLINE INTERDEPENDENCE

The emphasis here is scramjet engine/airframe integration methodology, and thus the focus is on the propulsion flowpath; however, the remainder of the vehicle cannot be ignored in the design of the flowpath because of the strong couplings that reflect throughout in hypersonic airbreathing vehicle designs. Figure 19 illustrates the complex interdependence among the disciplines in airbreathing hypersonic vehicle design (ref. 41). For example, aerodynamic's input surface coordinates from geometry; interacts with propulsion in defining the entire vehicle configuration; outputs heat loads to the thermal management analysis; outputs forces and temperatures to structures; and iterates with the trajectory to yield flight conditions, forces, and moments. As noted previously, not only are there a large number of couplings, but the sensitivities are high and the system is highly nonlinear. Thus, resolution requires a high degree of accuracy with all disciplines involved.

5.1 Automation/Optimization

In order to automate the design process and to be sure to capture all the interaction, a working environment for the multidisciplinary design, analysis, and optimization of airbreathing hypersonic vehicles (HOLIST) is being developed by SAO (ref. 41) in part through a contract with McDonnell Douglas (ref. 42). D.H. Petley is coordinating the effort. The implementation of HOLIST in SAO is being performed by J.G. Martin, an NPS contractor to SAO. HOLIST will help eliminate disconnects between disciplines, enable rapid multidisci-

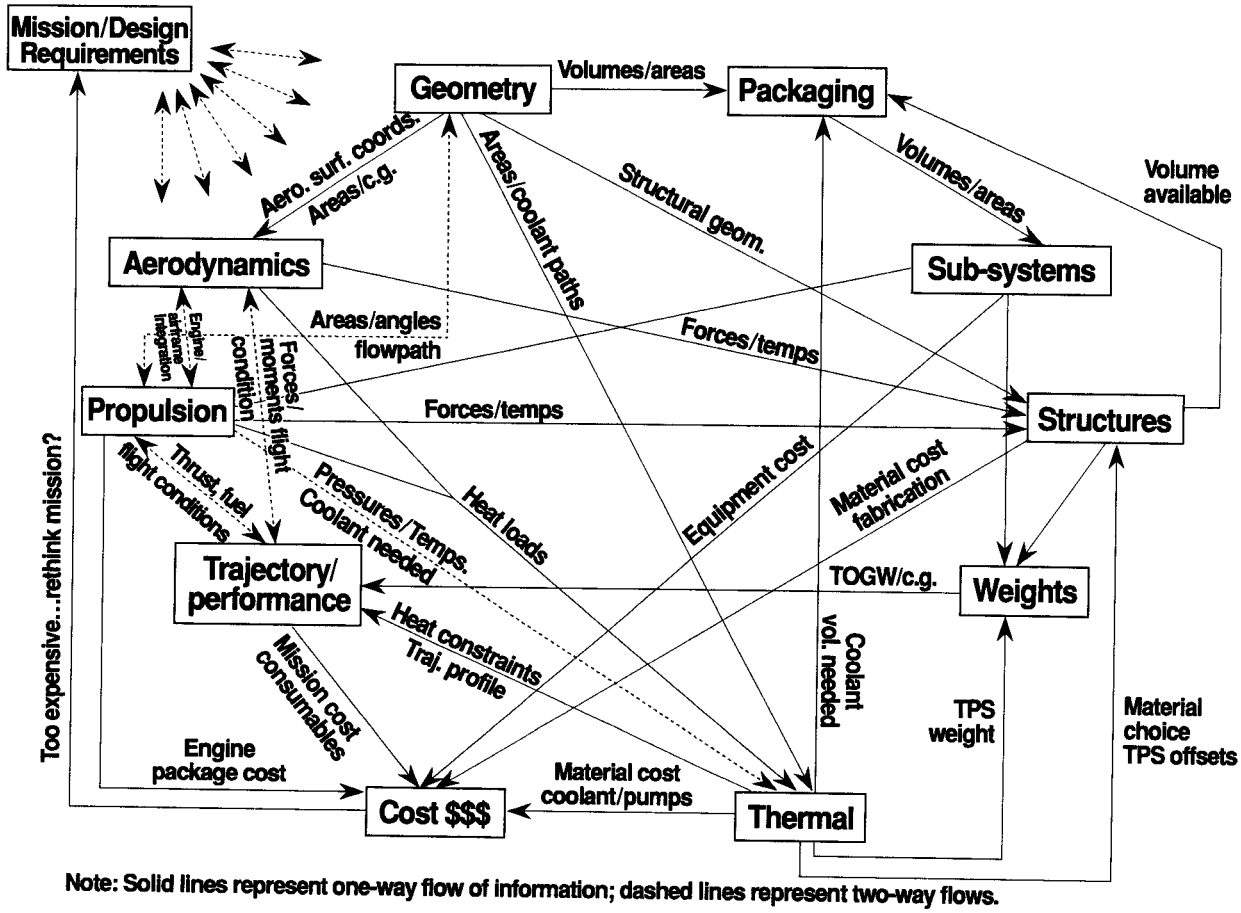

Figure 19. Discipline interdependence.

plinary parametrics, allow the evaluation of design sensitivities, and will enable the optimization of the vehicle design and trajectory. Currently a parametric geometry model, Pro/ENGINEER (ref. 20), is being incorporated into HOLIST. This will enable the entire vehicle configuration to be represented with a number of specified design variables. HOLIST is constructed modularly such that when improvements are made in any of the discipline tools, or new tools are available, these can be easily incorporated. A user-friendly optimizer, Optdes-X (ref. 43), has been integrated into the environment, and the entire system is set up on workstations, complete with graphical user interfaces.

Figure 20 is a simplified flowchart illustrating how an optimization proceeds in HOLIST. In the upper left-hand corner, the process set-up includes defining the design variables, objective function, constraints and convergence criteria for a run. The baseline vehicle geometry and packaging, together with a definition of the mass and thermo properties, follow. Analysis of the configuration proceeds with aerodynamics, propulsion, etc. (Note that for simplification of the diagram, several disciplines are not represented here, including structures and thermal management, for example.) The analysis can either be performed in real time, i.e., by running an analysis code, or a database can be accessed to obtain the discipline results. It is important to note that there is more than just one result being passed through this flowchart. In other words, since the vehicle will fly some trajectory, matrices of aerodynamic and propulsion data representing the coefficients of lift, drag, and thrust, and fuel flow rate, for example, at appropriate values of angle of attack and Mach number, must be passed through the loop. In addition, the propulsion flowpath geometry may vary along a trajectory requiring multiple geometry definitions.

Once the analyses are completed, the vehicle is flown as represented by the "Analyze Mission" box. From the mission results, the vehicle is sized. (It is also possible to define a scaling factor as a variable and use $|PFR-PFA| \leq .1$ as a constraint. This would eliminate the need to perform the sizing process in the extra loop.) At this point, if only a single vehicle analysis were required, the process would be complete. However, if it is desired to optimize the vehicle, the optimization process begins. Finite differences are used to calculate the derivatives of the objective function with respect to each of the design variables. Thus, for the perturbation of each design variable, one pass through the loop is made. Based on the derivative information, the vehicle design for the next iteration is defined. The objective function for the new design is evaluated, the derivatives at the new point in the design space are determined, and the process continues with the vehicle definition for the next iteration. Iterations continue until convergence criteria and all the constraints are satisfied, yielding the optimum vehicle configuration.

6. SUMMARY

The development of the scramjet engine/airframe integration methodology has progressed to a degree that allows resolution of hypersonic airbreathing vehicle designs for space access vehicles, cruise airplanes, and missiles for the dual-mode-ramjet flowpath segment of the design. The challenges ahead lie in reducing the turn-around time required with the application of this methodology in the hypersonic airbreathing vehicle design process, in refinement/implimentation of low speed aero/ propulsion integration methods, and in the development and automation of multidiscipline design processes. As these design processes mature, viable space access and hypersonic cruise airbreathing vehicle designs will evolve.

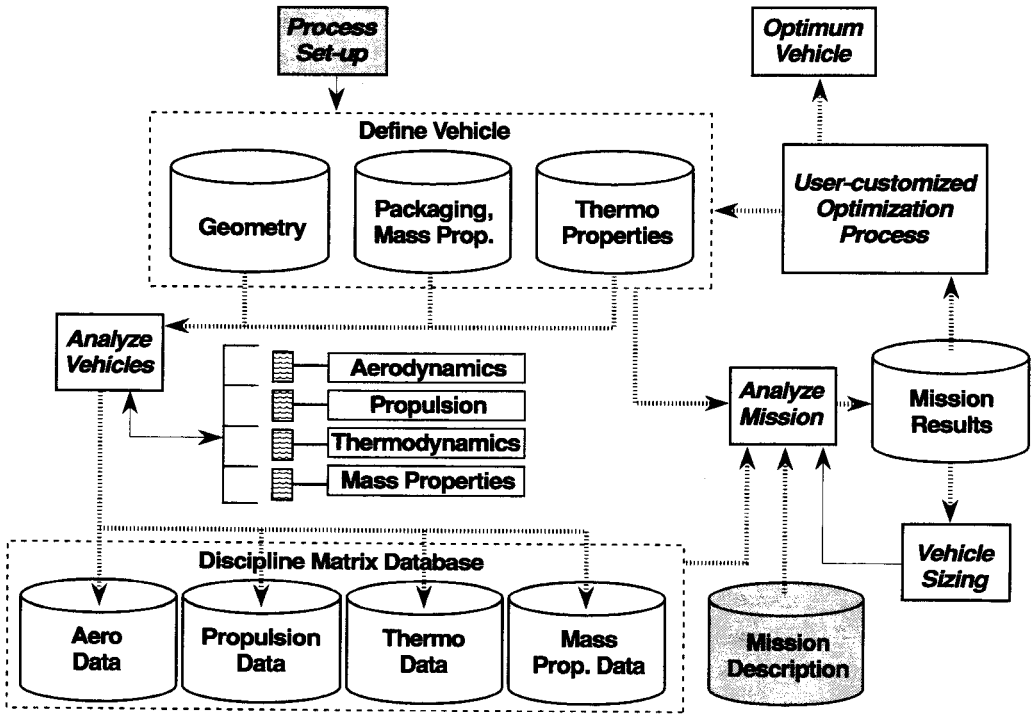

Figure 20. HOLIST design optimization.

7. REFERENCES

1. Hunt, J. L.; Lockwood, M. K.; Petley, D. H.; and Pegg, R. J.: Hypersonic Airbreathing Vehicle Visions and Enhancing Technologies. Presented at the 1997 STAIF Conference, Albuquerque, NM, January 26-30, 1997.

2. Pinckney, S. Z. and Walton, J. T.: Program SRGULL: An Advanced Engineering Model for the Prediction of Airframe-Integrated Subsonic/Supersonic Hydrogen Combustion Ramjet Cycle Performance. NASP TM-1120, January 1991.

3. McClinton, C. R.; Bittner, R.; and Kamath, P.: CFD Support of NASP Design. AIAA 90-5249, presented at the AIAA Second International Aerospace Planes Conference, Orlando, Florida , October 29-31, 1990,.

4. Pinckney, S. Z.: Isolator Modeling for Ramjet and Ramjet/Scramjet Transition. National Aero-Space Plane Technology Review, Paper Number 171, 1993.

5. Salas, M. D.: Shock Fitting Method for Complicated Two-Dimensional Supersonic Flows. Vol. 14, No. 5 in AIAA Journal, May 1976.

6. Spradley, L. W.; Robertson, S. J.; Mahaffey, W. A.; and Lohner, R.: The Solution Adaptive Modeling (SAM) CFD Software System. RSI 96-002, September 1996.

7. Lohner, R., et. al.: Fluid-Structure Interaction Using a Loose Coupling Algorithm and Adaptive Unstructured Grids. AIAA 95-2259, San Diego, California, June 1995.

8. Bogar, T. J.; Alberico, J. F.; Johnson, D. B.; Espinosa, A. M.; and Lockwood, M. K.: Dual-Fuel Lifting Body Configuration Development. AIAA 96-4592, Norfolk, Virginia, November 1996.

9. Pinckney, S. Z.: Turbulent Heat-Transfer Prediction Method for Application to Scramjet Engines. NASA TN D-7810, November 1974.

10. Pinckney, S. Z.: Flat-Plate Compressible Turbulent Boundary-Layer Static Temperature Distribution with Heat Transfer. Presented at AIAA Fifth Aerospace Sciences Meeting, New York, New York, January 23-25, 1967.

11. Schlichting, H.: Boundary Layer Theory. Pargamon Press, 1955.

12. Nestler, D. E.: Survey of Theoretical and Experimental Determinations of Skin Friction in Compressible Boundary Layers: Part I. The Laminar Boundary Layer on a Flat Plate. Thermodynamics Technical Memorandum No. 100, September 29, 1958.

13. Neal, L., Jr. and Bertram, M. H.: Turbulent-Skin-Friction and Heat-Transfer Charts Adapted from the Spalding and Chi Method. NASA TN D-3969, 1967.

14. Nestler, D. E.: Survey of Theoretical and Experimental Determinations of Skin Friction in Compressible Boundary Layers: Part II. The Turbulent Boundary Layer on a Flat Plate. Thermodynamics Technical Memorandum No. 109, January 29, 1959.

15. Murry, A. L.: Further Enhancements of the BLIMP Computer Code and User's Guide. Air Force Wright Aeronautical Labs, AFWAL-TR-88-3010, June 1988.

16. Petley, D. H.; Jones, S. C.; and Dziedzic, W. M.: Integrated Numerical Methods for Hypersonic Aircraft Cooling Systems Analysis. AIAA 92-0254, Reno, Nevada, January 6-9, 1992.

17. Anon.: SINDA '85/FLUINT User's Manual. Denver Aerospace Division of Martin Marietta Corp., Denver, Colorado, November 1987.

18. Petley, D. H. and Yarrington, P.: Design and Analysis of the Thermal Protection System for a Mach 10 Cruise Vehicle. Presented at the 1996 JANNAF Propulsion & Joint Subcommittee Meeting, Albuquerque, New Mexico, December 9-13, 1996.

19. Hunt, J. L.: Airbreathing/Rocket Single-Stage-to-Orbit Design Matrix. AIAA 95-6011, Chattanooga, Tennessee, April 3-7, 1995.

20. Parametric Technology Corporation: Pro/ENGINEER Fundamentals. Release 17.0.

21. Reymond, M. and Miller, M. of the McNeal-Schwendler Corporation: MSC/NASTRAN—Quick Reference Guide. Version 69.

22. PDA Engineering, PATRAN Division: P3/PATRAN User Manual. Vol. 1, Part 1: Introduction to PATRAN 3 and Part 2: Basic Fundamentals. Publication No. 903000, 1993.

23. Parametric Technology Corporation: Pro/MECHANICA™ Installation Guide. Release 17.0, August 1996.

24. Collier, C.: Thermoelastic Formulation of Stiffened, Unsymmetric Composite Panels for Finite Element Analysis of High Speed Aircraft. Paper 94-1579, 1994.

25. Collier, C.: Structural Analysis and Sizing of Stiffened, Metal Matrix Composite Panels for Hypersonic Vehicles. AIAA 92-5015, 1992.

26. Walters, R. W.; Cinnella, P.; Stack, D. C.; and Halt, D.: Characteristics Based Algorithms for Flows in Thermo-Chemical Nonequilibrium. AIAA 90-0393, January 1990.

27. Walters, R. W.: GASP - A Production Level Navier-Stokes Code Including Finite-Rate Chemistry. Proceedings of the Fourth Annual Meeting of the Center for Turbomachinery and Propulsion Research, April 1990.

28. Jentink, T. N.: An Evaluation of Nozzle Relaminarization Using Low Reynolds Number k- e Turbulence Models. AIAA 93-0610, Reno, Nevada, January 11-14, 1993.

29. Lam, C. K. G. and Bremhorst, K.: A Modified Form of the k- ε Model for Predicting Wall Turbulence. Transactions of the ASME, Vol. 103, pp. 456-460, September 1981.

30. Chien, K.: Predictions of Channel and Boundary-Layer Flows with a Low-Reynolds Number Turbulence Model. AIAA Journal, pp. 33-38, January 1982.

31. Srinivasan, S.; Bittner, R. D.; and Bobskill, G. J.: Summary of the GASP Code Application and Evaluation Effort for Scramjet Combustor Flowfields. AIAA 93-1973, Monterey, California, June 28-30, 1993.

32. Mekkes, G. L.: Computational Analysis of Hypersonic Shock Wave/Wall Jet Interaction. AIAA 93-0604, January 11-14, 1993.

33. Srinivasan, S. and Erickson, W. D.: Influence of Test Gas Vitiation on Mixing and Combustion at Mach 7 Flight Conditions. AIAA 94-2816, June 27-29, 1994.

34. MacDaniel, J. M.; Fletcher, D.; Hartfield, R.; and Hollo, S.: Staged Transverse Injection into Mach 2 Flow Behind a Rearward Facing Step: A 3-D Compressible Test Case for Hypersonic Combustion Code Validation. AIAA 91-5071, December 1991.

35. Rogers, R. C.; et. al.: Quantification of Scramjet Mixing in the Hypervelocity Flow of a Pulse Facility. AIAA 94-2518, June 1994.

36. McClinton, C. R.: Comparative Flowpath Analysis and Design Assessment of an Axisymmetric Hydrogen Fueled Scramjet Flight Test Engine at a Mach Number of 6.5. AIAA 96-4571, November 1996.

37. Kamath, P. S.; Mao, M.; and McClinton, C. R.: Scramjet Combustor Analysis with the SHIP3D PNS Code. AIAA 91-5090, 1991.

38. Kamath, P. S. and Mao, M.: Computation of Transverse Injection Into a Supersonic Flow with the SHIP3D PNS Code, AIAA 92-5062, 1992.

39. Braaten, M. E.: Development and Evaluation of Direct and Iterative Methods for the Solution of Equations Governing Recirculating Flows. Ph.D. Thesis, University of Minnesota, 1985.

40. Kamath, P. S.; Mao, M.; and McClinton, C. R.: A Parametric Study of Scramjet Combustors for Mach 8 to Mach 20 Flight. AIAA 91-1412, June 24-26, 1991.

41. Lockwood, M. K.; Petley, D. H.; Hunt, J. L.; and Martin, J. G.: Airbreathing Hypersonic Vehicle Design and Analysis Methods. AIAA 96-0381, Reno, Nevada, January 15-18, 1996.

42. Alberico, J.: The Development of an Interactive Computer Tool for Synthesis and Optimization of Hypersonic Airbreathing Vehicles. AIAA 92-5076, Orlando, Florida, December 1-4, 1992.

43. Design Synthesis, Inc.: OptdesX—A Software System for Optimal Engineering Design Users Manual. Release 2.0.3, 1994.